Development of Coldspray Ionization Mass Spectrometry (CSI-MS) and Its Application to Labile Organometallic Compounds in Solution

Kentaro Yamaguchi and Shigeru Sakamoto

Chemical Analysis Center, Chiba University

Coldspray ionization (CSI) mass spectrometry (MS) has been developed and applied to characterize labile organometallic compounds. While conventional ESI is not applicable to those compounds because of their instability to heat and/or air, CSI affords multiply charged molecular ions with many solvents molecules attached. Here we describe the CSI method and its application to several labile organometallic compounds.

Introduction

Many analytical results obtained by electrospray ionization mass spectrometry (ESI-MS) have been reported since the applicability of ESI to biomolecules and polymers was presented by Fenn et al. in 1989 [1]. Although characterization of labile organometallic compounds was also attempted by using ESI, molecular ions were not detected in most cases because of their instability. Even if the molecular ions are observed by using this ionization method, many fragment ions generated by thermal decomposition also appear in the mass spectrum. The heat given off from the desolvation chamber was thought to be necessary for ionization in the conventional ESI [2]. However, we developed coldspray ionization MS, a variant of ESI-MS operating at low temperature, in order to detect labile organometallic compounds [3].

In this report, we describe our new method, coldspray ionization mass spectrometry (CSI-MS), which allows easy and precise characterization of labile organometallic compounds in solution.

Coldspray Ionization Mass Spectrometry (CSI-MS)

Figure 1 shows the CSI apparatus, which consists of an electrospray or ion spray ionization probe and a desolvation chamber operating at low temperature. It features a drying gas (N_2) cooling device to maintain the temperature of the capillary and spray itself below –20°C, in order to promote ionization based on increased polarizability of the compounds caused by the higher dielectric constant at low temperature. The dielectric polarization (**P**) is a function of vacuum permittivity (ϵ_o), relative permittivity or dielectric constant (ϵ_ρ) and electric field (**E**).

$$\mathbf{P} = \epsilon_o (\epsilon_\rho - 1)\mathbf{E} \qquad \text{(eq. 1)}$$
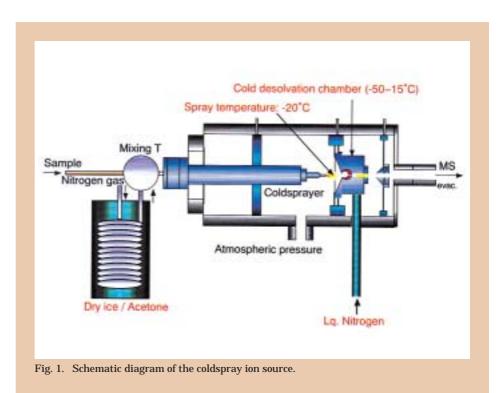
Generally, higher dielectric constant of solvents is observed at low temperature, as described in eq. 2 (T: temperature, θ: constant).

$$\epsilon_\rho = \epsilon_o \mathbf{e}^{-T/\theta} \quad \text{(eq. 2)}$$

Therefore, it should be possible to ionize thermally unstable ionic metal complexes by solvation without decomposition.

The ion source block and the desolvation chamber are also held at low temperature (–50 to 15°C) by pouring liquid nitrogen directly onto them, in order to allow transfer of unstable ions to the mass analyzer without decomposition.

Though desolvation by using a heated capillary and/or drying gas is thought to be an important step for ionization in the conventional ESI process, we confirmed that solvation (promoting electrolytic dissociation to form molecular ions) is a critical step in the

Fig. 1. Schematic diagram of the coldspray ion source.

Yayoi-cho, Inage-ku, Chiba 263-8522, Japan
E-mail : yamaguchi@cac.chiba-u.ac.jp

CSI process.

Characterization of Self-assembling Nano-sized Structures

Highly ordered supramolecules such as catenanes, rotaxanes, molecular capsules and molecular necklaces, derived by self-assembly on transition metals, have unique structures and properties [4]. Characterization of this class of metal complexes has generally been done with X-ray crystallography and NMR spectroscopy. However, it is often difficult to obtain a single crystal of sufficient quality for precise structure determination. Further, if molecules contain paramagnetic metals and/or exhibit fast exchange among plural structures, NMR spectroscopy can provide only limited structural information. As regards mass spectrometry, these compounds are usually unstable to the ionization impact or matrix reagents, even in the case of mild ionization methods such as fast atom bombardment (FAB), matrix-assisted laser desorption ionization (MALDI) and ESI. Even if the molecular ions are observed by using these ionization methods, many fragment ions also appear in the mass spectrum.

We adopted CSI-MS to characterize these self-assembling nano-sized structures in solution.
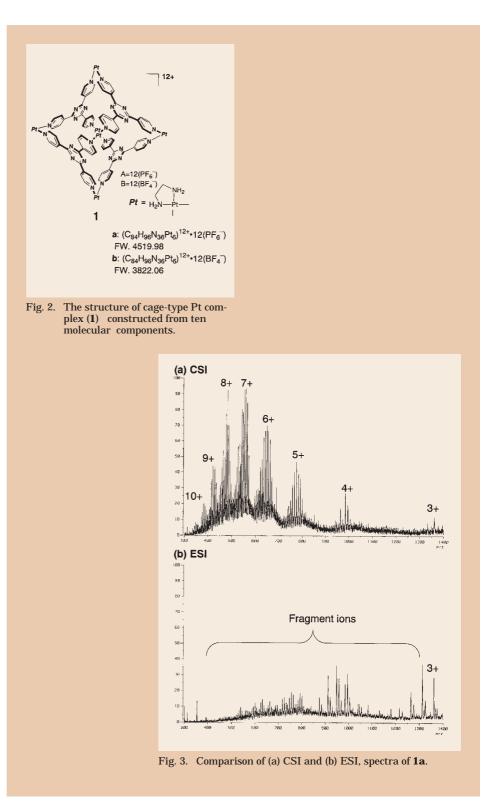
Experimental

Mass spectral measurements were performed with a four-sector (BE/BE) tandem mass spectrometer (JMS-700T, JEOL) equipped with the CSI source. Typical measurement conditions are as follows: acceleration voltage; 5.0 kV, needle voltage; 2.8 kV, needle current; 300 to 700 nA, orifice voltage; 20 to 70 V, resolution (10 % valley definition); 1000 to 5000, sample flow; 8 µL/min, solvent; acetonitrile (CH_3CN), concentration; 0.01 to 0.1 mmol/L, spray temperature, –20°C, ion source temperature; 10 °C.

Comparison Between CSI-and ESI-MS Spectra of Self-assembling Complexes

The CSI- and conventional ESI-MS spectra of a 0.1 mmol/L acetonitrile solution of complex **1a**, [5] constructed from ten molecular components (**Figure 2**) including six Pt(II)(en) and four rigid tridentate ligands, were compared (**Figure 3**). While a significant result was not obtained from the conventional ESI-MS (**Figure 3b**), presumably because of the high desolvation plate temperature (200 °C), multiply charged molecular ions of [**1a** – $(PF_6)_n + (CH_3CN)_m]^{n+}$ ($n = 3 – 10$, $m = 0 – 21$) were clearly observed without decomposition in the CSI-MS (**Figure 3a**). Interestingly, the number of acetonitriles (m) attached to the molecular ion increased with increasing positive charge (**Figure 4**). This suggests that the acetonitrile molecules solvated the Pt^{2+} ions. Thus, CSI was proved to be an effective method to characterize the solution structures of labile self-assembling complexes.

The Influence of Counter Anions

We also examined whether changing the counter anions would influence the intensity of the molecular ions in the CSI. The CSI-MS

Fig. 2. The structure of cage-type Pt complex (**1**) constructed from ten molecular components.

Fig. 3. Comparison of (a) CSI and (b) ESI, spectra of **1a**.

spectrum of complex **1b**, in which PF_6^- is replaced with BF_4^-, was measured. [K + CH_3CN]+ ($m/z = 80$), [Na + $2CH_3CN$]+ ($m/z = 105$) and the multiply charged molecular ions [**1b** – $(BF_4)_n + (CH3CN)_m]^{n+}$ ($n = 3 – 6$, $m = 0 – 7$) were again observed. However, the intensity of the molecular ions as well as the observed ion charges were clearly reduced compared with those of complex **1a**. This can perhaps be ascribed to the difference of coordination ability of PF_6^- and BF_4^- to Pt^{2+}. PF_6^- seems more favorable for the CSI process based on solvation, because the lower coordination ability of this anion may promote dissociation. Selection of the counter ion seems to be important.

High Resolution CSI-MS Measurement of Self-assembling Complexes

We found that some macrocyclic polyethers, crown ether compounds, exhibit excellent performance as internal calibrants for exact mass measurement in CSI-MS [6]. The reasons are as follows:
(1) Crown ethers with alkali metal ions (M= Na^+, K^+, Rb^+ and Cs^+) are easily ionized as [crown + M]+ under the CSI condition.
(2) Crown ethers exhibit no interference with the analyte when the sample solution contains various kinds of calibrants and

adducts.

(3) Essentially quantitative ionizing ability of crown ethers is observed in the positive CSI-MS process.

An exact mass measurement was performed by using crown ether compounds {[(dibiphenyl-22-crown-6) + K]$^+$; 551.1836 and [(dinaphthyl-24-crown-8) + Na]$^+$; 571.2308} as internal calibrants {[$\mathbf{1a}$ – 7(PF$_6$) + 10AN]$^{7+}$; obs. 559.2507, $calcd$. 559.2480} (**Figure 5**). As can be seen in Figure 5, the deviation in the measured mass number is less than 10 ppm for each compound. This result suggests the excellent utility of these crown ethers as internal calibrant in CSI-MS.

Characterization of Multiple-link Interlocking-type Cu(I)-Pd(II) Complex

The CSI-MS spectra of the multiple-link interlocking-type Cu(I)-Pd(II) complex $\mathbf{2}$, [7] constructed from ten molecular components including two Cu(I), four Pd(II)(en) and four ligands, were measured (**Figure 6**).

The CSI-MS spectrum of complex $\mathbf{2}$ at high concentration (4.2 mg / 1 mL in CH$_3$CN) exhibited monomeric $\mathbf{2}$ (Cu: Pd: Ligand = 2: 4: 4) {[$\mathbf{2}$ – (PF$_6$)$_n$ + (CH$_3$CN)$_m$]$^{n+}$ ($n = 3 – 5$, $m = 0$ – 1)} and dimeric $\mathbf{2}_2$ (Cu : Pd : Ligand = 4: 8: 8) {[($\mathbf{2}$)$_2$ – (PF$_6$)$_n$]$^{n+}$ ($n = 4 – 5$)} states in equilibrium. The observed mass numbers and isotopic patterns of the ion clusters, as well as the ion charges, match the theoretical values well (**Figure 6a**). In the case of diluted solution (x 20), the ion peaks of the dimeric ion peaks disappeared and multiply charged monomeric ions of [$\mathbf{2}$ – (PF$_6$)$_n$ + (CH$_3$CN)$_m$]$^{n+}$ ($n = 3 – 7$, $m = 0 – 8$) were observed in CSI-MS (**Figure 6b**). The ion peaks of the monomeric species diminished and a new ion peak ($m/z = 825$) formed by decomposition appeared in further diluted solution (×40) (**Figure 6c**). In even more diluted solution (×120), the ion peaks of the half-monomeric constitution [$\mathbf{2}_{1/2}$ – (PF$_6$)$_2$]$^{2+}$ as well as fragment ions generated by decomposition were observed, while the ion peaks of the monomeric species completely disappeared (**Figure 6d**). The change from monomeric to half-monomeric structure depending on the concentration is clearly observed in the different charge ratios of 4 + and 2 + at an identical ion peak m/z 930 (Figure 6). Finally, no significant ion peak other than fragment ions was observed in highly diluted solution (×200), suggesting disassembly of this compound (**Figure 6e**). Thus, CSI-MS was proved to be a powerful tool for analyzing the equilibria of multiple-link self-assembling catenanes in solution.

Characterization of Box-type Pd Complex

The trimeric box-type Pd complex $\mathbf{3}$ [8] was constructed from nine components including six Pd(II)(en) and four ligands in water. The structure of complex $\mathbf{3}$ was characterized by means of NMR and CSI-MS (**Figure 7**). ^{1}H-NMR spectra suggested several different box-type Pd complexes in CD$_3$CN. The dynamic behavior of the coordination boxes in solution was monitored by CSI-MS. When the components of the complex were dissolved in CH$_3$CN, trimeric molecular ions, $\mathbf{3}^{2+}$, $\mathbf{3}^{3+}$, $\mathbf{3}^{4+}$ and $\mathbf{3}^{5+}$ were immediately formed (**Figure 8a**). After 0.5 h, the CSI-MS clearly showed the

formation of $\mathbf{3}$, $\mathbf{4}$ (tetramer) and $\mathbf{5}$ (pentamer). After 2 h, CSI-MS showed an increase of $\mathbf{4}$ and $\mathbf{5}$ and a decrease of $\mathbf{3}$. After 5 h, two major components, $\mathbf{4}$ and $\mathbf{5}$, were observed. After 26 h, the only major component is the tetrameric box $\mathbf{4}$ as observed by CSI-MS. Thus, the dynamic behavior of the coordination boxes in solution was clearly shown by CSI-MS.

Constitution of Grignard Reagent RMgCl in Tetrahydrofuran

The constitutional investigation of Grignard reagents, discovered in 1900, has been extremely challenging. Although the Schlenk equilibrium is generally accepted to interpret the structure of RMgX, our knowledge of the real species in solution is still limited. We recently presented evidence suggesting that RMg$_2$(μ – Cl$_3$) is the dominant species in the case of RMgCl in THF solution. Ashby and Beckr [9], Toney and Stucky[10] and Sobota and Duda [11] also suggested this constitution as a dominant species in the case of RMgCl in THF. However, in all cases the evidence was rather indirect. Therefore, we investigated the constitution of RMgCl by means of CSI-MS and tandem mass spectrometry (MS/MS).

Experimental

CSI-MS spectrum measurement was performed with a four-sector (BE/BE) tandem mass spectrometer (JMS-700T, JEOL) equipped with the CSI source. Typical measurement conditions are as follows: <CSI-MS> acceleration voltage; 5.0 kV, needle voltage; 2.8 kV, needle current; 300 – 700 nA, orifice voltage; 50 V, resolution (10 % valley definition); 1000, sample flow; 33 μL/min, solvent; dry THF, concentration; 10 mmol/L, spray temperature, –20°C, ion source temperature; 10°C. <MS/MS> acceleration voltage; 5.0 kV, collision gas; Xe, collision cell voltage; 0 V.

Structure of MeMgCl in THF

In the mass spectrum of MeMgCl in THF solution, three major ion peaks, m/z 457, 529 and 601, were clearly observed (**Figure 9a**). We examined the compositions of these ions, using MS/MS and compared the calculated and observed isotopic patterns. It is apparent that these species include plural solvent molecules and an Mg$_2$Cl$_3$ component (**Figure 9b**). Therefore, the ions m/z 457, 529 and 601 obtained from MeMgCl were assigned as [MeMg$_2$Cl$_3$ (THF)$_4$ – H]$^+$,[MeMg$_2$Cl$_3$ (THF)$_5$ – H]$^+$ and [MeMg$_2$Cl$_3$ (THF)$_6$ – H]$^+$, respectively, pointing to the involvement of MeMg$_2$(μ – Cl$_3$) (THF)$_{4-6}$.

We concluded that the trimeric constitution, RMg$_2$(μ – Cl$_3$) is a major species in the case of RMgCl in THF [12].
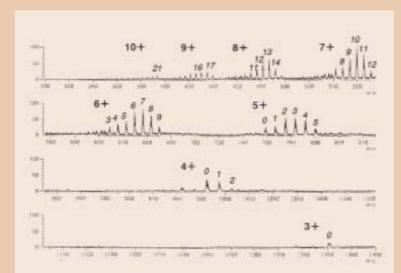
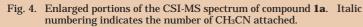$$3RMgCl \rightleftarrows R_2Mg + RMg_2Cl_3$$

Summary

CSI-MS has been developed and applied to characterize the solution structures of various abile organometallic compounds. This method allows easy and precise characterization of labile self-assembling nano-sized complexes. CSI-MS also revealed the constitution

of RMgCl in THF. Further, we recently reported that the CSI-MS is applicable to investigate solution structures of biomolecules [13].

References

1. Fenn, J. B., Mann, M., Meng, C. K., Wong, S. F. and Whitehouse, C. M.: Electrospray ionization for mass spectrometry of large biomolecules, *Science*, **246**, 64-71 (1989)

2. Kebarle, P. and Tang, L.: From ions in solution to ions in the gas phase, *Anal Chem.*, **65**, 972A-986A (1993)

3. Sakamoto, S., Fujita, M., Kim, K. and Yamaguchi, K.: Characterization of self-assembling nano-sized structures by means of coldspray ionization mass spectrometry, *Tetrahedron*, 56, 955-964 (2000)

4. Fujita, M.: Metal-directed self-assembly of two- and three-dimensional synthetic receptors, *Chem. Soc. Rev.*, **27**, 417-425 (1998).

5. Fujita, M., Oguro, D., Miyazawa, M., Oka, H., Yamaguchi, K. and Ogura, K.: Self-assembly of ten molecules into nanometre-sized organic host frameworks, *Nature*, **378**, 469-471 (1995)

6. Yamaguchi, K., Sakamoto, S., Imamoto, T. and Ishikawa, T.: Internal calibrant for an exact mass measurement in electrospray ionization mass spectrometry, *Anal Sci.*, **15**, 1037-1038 (1999)

7. Ibukuro, F., Fujita, M., Yamaguchi, K. and Sauvage, J.-P.: Quantitative and spontaneous formation of a doubly interlocking [2] catenane using copper (I) and palladium (II) as templating and assembling centers, *J. Am. Chem. Soc.*, **121**, 11014-11015 (1999)

8. Yamanoi, Y., Sakamoto, Y., Kusukawa, T., Fujita, M., Sakamoto, S. and Yamaguchi, K.: Dynamic assembly of coordination boxes from (en)Pd(II) unit and a rectangular panel-like ligand: NMR, CSI-MS and X-ray Study, *J. Am. Chem. Soc.*, **123**, 980-981 (2001)

9. Ashby, E. C. and Becker, W. E.: Concerning the structure of the Grignard reagent, *J. Am. Chem. Soc.*, **85**, 118-119 (1963)

10. Toney, J. and Stucky, G. D.: The stereochemistry of polynuclear compounds of the main group elements. [C$_2$H$_5$Mg$_2$Cl$_3$ (C$_4$H$_8$O)$_3$]$_2$, a tetrameric Grignard reagent, *J. Organomet. Chem.*, **28**, 5-20 (1971)

11. Sobota, P. and Duda, B.: Influence of MgCl$_2$ on Grignard reagent composition in tetrahydrofuran. III, *J. Organomet. Chem.*, **332**, 239-245 (1987)

12. Sakamoto, S., Imamoto, T. and Yamaguchi, K.: Constitution of Grignard reagent RMgCl in tetrahydrofuran, *Org. Lett.*, **3**, 1793-1795 (2001)

13. Kunimura, M., Sakamoto, S. and Yamaguchi, K.: Alkali metal-mediated proline aggregation in solution observed by coldspray ionization mass spectrometry, *Org. Lett.*, in press.
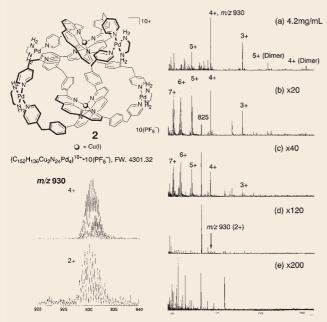
Fig. 4. Enlarged portions of the CSI-MS spectrum of compound **1a**. Italic numbering indicates the number of CH₃CN attached.

Fig. 5. High-resolution CSI-MS spectrum of compound **1a** with exact mass number.

[1a–7(PF₆)+10AN]⁷⁺
obs. 559.2507
calcd. 559.2480
deviation −2.7mmu, 4.8ppm

Fig. 6. The structure of double-interlocking type Cu-Pd complex (**2**) and CSI-MS spectra of compound **2** at various concentrations: (a) 4.2 mg/mL, (b) 320, (c) 340, (d) 3120 and (e) 3200.
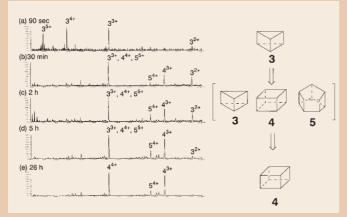

Fig. 7. The structure of box type Pd complex (**3**) (trimer) and the CSI-MS spectrum of compound **3** in solution.

Fig. 8. CSI-MS spectra of box-type Pd complex (**3**) in CH₃CN at various time points: (a) 90 sec, (b) 0.5 h, (c) 2 h, (d) 5 h and (e) 26 h, after dissolution.
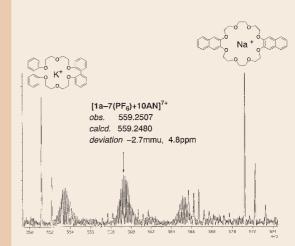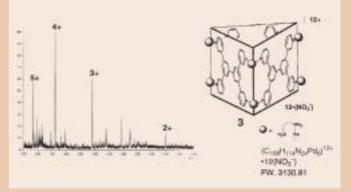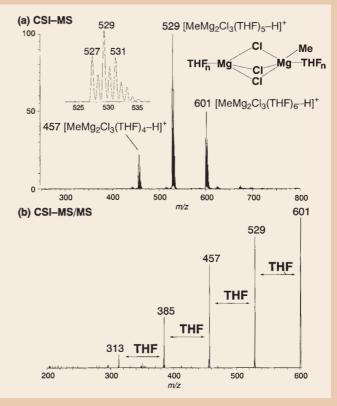

Fig. 9. (a) CSI-MS spectrum of MeMgCl in THF and (b) product ion spectra of *m/z* 601.